Highly Anisotropic Luminescence from Poly(9,9-dioctylfluorene) Nanowires Doped with Orientationally Ordered β-Phase Polymer Chains

Deirdre O'Carroll[†] and Gareth Redmond*[,‡]

Tyndall National Institute, Lee Maltings, Prospect Row, Cork, Ireland

Received June 9, 2008. Revised Manuscript Received August 18, 2008

We quantitatively assess the nature and extent of emissive polymer chain organization within individual poly(9,9-dioctylfluorene) nanowires fabricated by solution-assisted template wetting. A minority fraction of planar, extended β-phase polymer chains occurs within the nanowires, which dominates their luminescence behavior. Nanowires exhibit pronounced optical birefringence and detailed polarized optical microscopy analysis indicates preferential axial alignment of polymer chains. Polarization-resolved near-field photoluminescence imaging and spectroscopy methods are employed to probe local spatial variations in light emission intensity along individual nanowires. Data indicate strong axially polarized nanowire emission, with locally measured dichroic ratios up to 8.9, consistent with preferential axial alignment of emissive β-phase polymer chains. To visualize the extent of β-phase chain alignment within a typical nanowire, we generated image maps of the orientational order parameter, $\langle P_2 \rangle$, from measured near-field emission intensity image data. Numerous domains of long-range order up to 2 μm in size with $\langle P_2 \rangle$ values ranging from 0.47 to 0.76 are identified, indicating extensive axial alignment of emissive β-phase chains within the nanowires. Poly(9,9-dioctylfluorene) nanowires exhibiting micrometer-scale order make them attractive elements for future subwavelength organic opto-electronic devices.

Introduction

Inorganic semiconductor nanowires are widely studied with respect to their potential for use in ultraminiaturized electronic and photonic technologies.[1,2] The vapor−liquid−solid epitaxy technique has been recognized as a powerful method for the synthesis of single-crystalline inorganic nanowires with controlled diameters and lengths.[3] In addition, control over crystallographic growth direction is very desirable for optimization of nanowire-based devices. This is particularly relevant for important photonic and electronic materials such as gallium nitride (GaN), zinc oxide (ZnO) and silicon, all of which exhibit anisotropic crystal structures, because key parameters such as photoluminescence (PL) polarization state, index of refraction, nonlinear optical activity, thermal and electrical conductivity, and piezoelectric polarization largely depend on the orientations of optical or electrical dipoles within the materials.[2,4−7] For example, depending on the orientation of the optical axis of the crystal with respect to the growth axis in GaN and ZnO nanowire lasers, bound cavity modes can experience differences in optical gain depending on the polarization state of each mode.[4] Also, the thermal conductivity of [110]-oriented GaN nanowires has been predicted to be substantially lower than that of [001]-oriented wires.[5] Therefore, the choice of crystallographic growth direction, relative to the nanowire long axis, must be carefully considered.[1,8]

In organic semiconductor nanowires, molecular orientation is also critical to the control and tuning of physical properties since optical and electrical dipole orientations are generally intrinsically polarized along the molecular chain axis.[9−14] Control of molecular orientation in organic nanostructures may be achieved by tuning material processing parameters such as molecular weight, solvent type, or anneal temperature.[15,16] Recently, organic nanowires based on the well-

* Corresponding author. E-mail: gareth.redmond@ucd.ie.
[†] Current address: Thomas J. Watson Laboratory of Applied Physics, California Institute of Technology, 1200 E. California Blvd., MC 128-95, Pasadena, CA 91125.
[‡] Current address: School of Physics and School of Chemistry and Chemical Biology, University College Dublin, Belfield, Dublin 4, Ireland.

(1) Li, Y.; Qian, F.; Xiang, J.; Lieber, C. M. *Mater. Today* **2006**, *9*, 18.
(2) Sirbuly, D. J.; Law, M.; Yan, H.; Yang, P. *J. Phys. Chem. B* **2005**, *109*, 15190.
(3) Yang, P.; Yan, H.; Mao, S.; Russo, R.; Johnson, J.; Saykally, R.; Morris, N.; Pham, J.; He, R.; Choi, H.-J. *Adv. Funct. Mater.* **2002**, *12*, 323.
(4) Johnson, J. C.; Yan, H.; Yang, P.; Saykally, R. J. *J. Phys. Chem. B* **2003**, *107*, 8816.
(5) Wang, Z.; Zu, X.; Gao, F.; Weber, W. J.; Crocombette, J.-P. *Appl. Phys. Lett.* **2007**, *90*, 161923.
(6) Long, J. P.; Simpkins, B. S.; Rowenhorst, D. J.; Pehrsson, P. E. *Nano Lett.* **2007**, *7*, 831.
(7) Wang, Z. L. *J. Phys.: Condens. Matter* **2004**, *16*, R829.
(8) Ng, H. T.; Han, J.; Yamada, T.; Nguyen, P.; Chen, Y. P.; Meyyappan, M. *Nano Lett.* **2004**, *4*, 1247.
(9) Campoy-Quiles, M.; Etchegoin, P. G.; Bradley, D. D. C. *Phys. Rev. B* **2005**, *72*, 045209.
(10) Yao, H.; Domoto, K.; Isohashi, T.; Kimura, K. *Langmuir* **2005**, *21*, 1067.
(11) Heliotis, G.; Xia, R.; Whitehead, K. S.; Turnbull, G. A.; Samuel, I. D. W.; Bradley, D. D. C. *Synth. Met.* **2003**, *139*, 727.
(12) Lebedenko, A. N.; Guralchuk, G. Y.; Sorokin, A. V.; Yefimova, S. L.; Malyukin, Y. V. *J. Phys. Chem. B* **2006**, *110*, 17772.
(13) Yanagi, H.; Okamoto, S. *Appl. Phys. Lett.* **1997**, *71*, 2563.
(14) Sirringhaus, H.; Brown, P. J.; Friend, R. H.; Nielsen, M. M.; Bechgaard, K.; Langeveld-Voss, B. M. W.; Spiering, A. J. H.; Janssen, R. A. J.; Meijer, E. W.; Herwig, P.; de.Leeuw, D. M. *Nature* **1999**, *401*, 685.
(15) Chen, P.; Yang, G.; Liu, T.; Li, T.; Wang, M.; Huang, W. *Polym. Int.* **2006**, *55*, 473.

10.1021/cm8015534 CCC: $40.75
Published on Web 09/30/2008

known blue-light-emitting conjugated polymer poly(9,9-dioctylfluorene), PFO, were fabricated by the method of melt-assisted wetting of porous anodic alumina templates. These nanowires exhibited clear molecular orientation-dependent optical properties whereby radial internal alignment of the emissive polymer molecules within the wires facilitated propagation of photoluminescence along each nanowire long axis with subsequent out-coupling at the wire ends.[17−19] As a result, key photonic functions such as active waveguiding, axial Fabry-Pérot microcavity effects, and optically pumped lasing were demonstrated in these wires.

In this paper, we study molecular organization in PFO nanowires fabricated by the alternative route of solution-assisted template wetting. Such nanowires consist primarily of the disordered glassy phase (g-phase) of PFO, in which the molecular chains exist in random conformations, along with a minority fraction of the β-phase of PFO, characterized by a distinct planar, extended-chain conformation.[20−23] This latter phase completely dominates the emission characteristics of the wires, likely as a result of ultrafast migration of excitons to the lower-energy β-phase segments.[24,25] In this work, polarized optical techniques are employed to study the nature and extent of organization of the polymer molecules within individual solution-wetted PFO nanowires with high spatial resolution. The wires are found to exhibit pronounced optical birefringence when observed between crossed polarizers with detailed polarized optical microscopic analysis suggesting axial alignment of the polymer chains. The impact of this internal chain alignment on single nanowire emission is investigated using photoluminescence aperture near-field scanning optical microscopy and spectroscopy methods. Polarization-resolved near-field emission intensity images of single wires exhibit strongly anisotropic luminescence with a preferred axial polarization indicating that a significant number of the emissive polymer chains are preferentially oriented about the long axis of each nanowire. Corresponding polarization-resolved near-field emission spectra confirm that the emission anisotropy arises from the more planar, extended β-phase polymer chain conformation. Overall, it is demonstrated that solution-assisted template wetting provides a straightforward processing route to PFO nanowires that, because of strong internal orientational ordering of the emissive β-phase polymer chains across micrometer length scales, may successfully act as highly polarized, subwavelength photoluminescent light sources.

(16) Knaapila, M.; Stepanyan, R.; Lyons, B. P.; Torkkeli, M.; Monkman, A. P. *Adv. Funct. Mater.* **2006**, *16*, 599.
(17) O'Carroll, D.; Lieberwirth, I.; Redmond, G. *Nat. Nanotechnol.* **2007**, *2*, 180.
(18) O'Carroll, D.; Lieberwirth, I.; Redmond, G. *Small* **2007**, *3*, 1178.
(19) O'Carroll, D.; Redmond, G. *Physica E* **2008**, *40*, 2468.
(20) O'Carroll, D.; Iacopino, D.; O'Riordan, A.; Lovera, P.; O'Connor, E.; O'Brien, G. A.; Redmond, G. *Adv. Mater.* **2008**, *20*, 42.
(21) Grell, M.; Bradley, D. D. C.; Long, X.; Chamberlain, T.; Insbasekaran, M.; Woo, E. P.; Soliman, M. *Acta Polym.* **1998**, *49*, 439.
(22) Grell, M.; Bradley, D. D. C.; Ungar, G.; Hill, J.; Whitehead, K. S. *Macromolecules* **1999**, *32*, 5810.
(23) Ariu, M.; Lidzey, D. G.; Sims, M.; Cadby, A. J.; Lane, P. A.; Bradley, D. D. C. *J. Phys.: Condens. Matter* **2002**, *14*, 9975.
(24) Ariu, M.; Sims, M.; Rahn, M. D.; Hill, J.; Fox, A. M.; Lidzey, D. G.; Oda, M.; Cabanillas-Gonzalez, J.; Bradley, D. D. C. *Phys. Rev. B* **2003**, *67*, 195333.
(25) Kahn, A. L. T.; Sreearunothai, P.; Herz, L.; Banach, M. J.; Köhler, A. *Phys. Rev. B* **2004**, *69*, 085201.

Experimental Section

Nanowire Synthesis. Poly(9,9-dioctylfluorene) (PFO) material with weight-average molecular weight of 64 kDa or 80 kDa (polydispersity index 2.9 or 4.3, respectively; GPC, in tetrahydrofuran (THF) vs polystyrene standards) was purchased from American Dye Source, Inc. For nanowire synthesis, a drop of a PFO solution in THF (typically, 60 mg mL^{-1}) was deposited on a glass slide and a porous anodic alumina membrane/template (200 nm nominal pore size; Anodisc 13, Whatman Ltd.) was immediately brought in contact with the drop. A glass coverslip was pressed on top of the alumina template, and subsequently, a microscope slide was placed on top of the coverslip. A 2.5 kg weight was applied to the microscope slide for at least 16 h in order to maximize pore wetting by the PFO solution and to allow the THF solvent to slowly evaporate resulting in solidification of the polymer within the template pores. The high PFO solution concentration and slow solvent evaporation favored nanowire rather than nanotube formation. At the end of the process, the excess polymer was removed from the template surface using 1200 grit sand paper or a scalpel. Nanowires were liberated by soaking a filled template in sodium hydroxide (NaOH; 6 M) for at least 30 min. The resulting wire residue was rinsed thoroughly with deionized water and subsequently suspended in decane or isopropyl alcohol (IPA) by sonication (∼10−30 s). A pale yellow suspension of dispersed wires was obtained.

Optical Characterization. Optical images of PFO nanowires were acquired using an Axioskop II Plus epi-fluorescence microscope (Carl Zeiss, Inc.) equipped with two 100 W halogen lamps (for reflected light and transmitted light measurements) and a thermoelectrically cooled color CCD camera (DEI-750T, Optronics) and appropriate filter sets. Polarized optical microscope (POM) images were acquired using crossed polarizers and with the sample mounted on a rotatable translation stage to detect sample birefringence. A 550 nm λ-retardation plate was employed to establish the principle direction of alignment of the polymer chains in the wires.

Acid-cleaned glass coverslips were used as substrates for near-field PL measurements. In this regard, a nanowire coated glass coverslip was placed onto the motorized X−Y (∼1 μm resolution) stage of a modified transmission-mode aperture near-field scanning optical microscope (NSOM; Veeco Instruments Ltd.) and fixed in position using Scotch tape placed at each corner of the sample. For near-field photoexcitation, the output of a 405 ± 5 nm laser was directed into a single-mode optical fiber (FS-A, Newport Corp.), which was then butt-coupled with an NSOM probe fiber (i.e., an aluminum coated, tapered, single-mode, optical fiber probe with aperture radius of 50−80 nm; Veeco Instruments Ltd.); see Figure S1 in the Supporting Information. Nanowire PL was collected in the far-field using a 100× oil immersion objective (1.25 NA; Achrostigmat, Carl Zeiss, Inc.). Two avalanche photodiodes (APDs; SPCM-AQR-14, Perkin-Elmer, Inc.) were placed in the collection path along with a broadband polarizing cube beamsplitter (Melles Griot) for dual polarization PL image acquisition. Excitation light was rejected from the optical path using a long-pass filter placed before the cube beamsplitter. To measure polarization-resolved near-field PL spectra, we directed nanowire emission via a Glan-Thompson polarizer and an achromatic lens (75 mm focal length) into a 150 mm focal length imaging spectrometer (SP-150, Acton Research Corp.) equipped with a 300 g mm^{-1} grating and a liquid nitrogen cooled charge-coupled device (CCD; VersArray LN-512B, Princeton Instruments, Inc.). The PL light was centered and focused into the narrowed entrance slit (0.3 nm, i.e., 6.6 nm spectral resolution) of the spectrometer prior to spectral acquisition by monitoring the PL spot incident on the CCD array while making

small adjustments to the achromat. Prior to near-field excitation, a single, discrete PFO nanowire was located by acquiring NSOM topography images (shear force mechanism) with the excitation laser light switched off, to prevent unnecessary photodegradation of the polymer nanowire prior to acquiring the near-field PL data. To minimize probe-heating effects (drift and polymer degradation) during system alignment and data acquisition, excitation intensity from the NSOM probe was kept below 1000 counts ms^{-1} monitored at the APDs (i.e., <100 μW coupled into the NSOM probe fiber). The polarization state of the excitation light was set parallel to the long axis of a selected nanowire (determined in the far-field using the two APDs and with the long-pass filter flipped down) using a half- and quarter-wave plate combination in front of the laser, single-mode fiber paddles (Thorlabs, Inc.) and/or an in-line polarization controller (Newport Corp.) applied to the untapered end of the NSOM probe fiber. Linear excitation polarization ratios better than 7:1 were typically achieved using this method.

Results and Discussion

PFO nanowires doped with β-phase were synthesized by the method of solution-assisted template wetting, which has been described in detail elsewhere.[20,26−28] Briefly, upon contact between a porous alumina template and a droplet of PFO dissolved in tetrahydrofuran (THF; typically 60 mg mL^{-1}), the polymer solution penetrated the template by capillary action. Prolonged contact (>16 h) between the template and the solution resulted in the formation of PFO nanowires. Subsequently, the alumina template was dissolved in sodium hydroxide (NaOH). The length, width, and shape of the nanowires corresponded to that of the template pores. Statistical data for PFO nanowires extracted from scanning electron microscopy (SEM) images revealed an average nanowire diameter and length of 232 nm and 15 μm, respectively. After being rinsed with deionized water, nanowires were suspended in isopropyl alcohol (IPA) or decane by sonication. Mats of PFO nanowires were drop-deposited onto glass coverslips from suspension and allowed to dry.

Polarized optical microscopy (POM) was employed to investigate the possible existence of optical anisotropy in the nanowires, an indicator of internal molecular orientation. To this end, mats of PFO nanowires were formed on glass coverslips by drop-deposition from decane suspension followed by drying in air. Isolated single nanowires were also drop-deposited onto glass coverslips and aligned under nitrogen gas flow. Within the mats, the nanowires exhibited strong blue/white color contrast relative to the black background when placed between crossed polarizers in air, suggesting that the wires were birefringent; see Figure 1a. Such birefringence is typically observed in crystalline materials and in most stressed, stretched, or flow-aligned glasses and polymers as a result of a preferred direction of internal molecular alignment.[29,30] The inset of Figure 1a shows a typical epi-fluorescence image of a PFO nanowire mat on a glass substrate. Discrete, well-dispersed wires with uniform blue photoluminescence along the nanowire lengths were apparent with some degree of axial curvature, indicating the flexibility of these nanostructures. Figure 1b−d shows POM images of two crossed nanowires on a glass coverslip between crossed polarizers in air. Crossed nanowires were achieved by sequential deposition of nanowires under nitrogen gas flow in orthogonal directions. Optimum brightness (i.e., maximum contrast) occurred when the nanowires were positioned at either 45 or 135° to the crossed polarizers (Figure 1b) and extinction (i.e., minimum contrast) occurred when the nanowires were positioned in either parallel or perpendicular orientations with respect to the crossed polarizers, consistent with uniaxial alignment of the polymer chains within the wires; see Figure 1c.

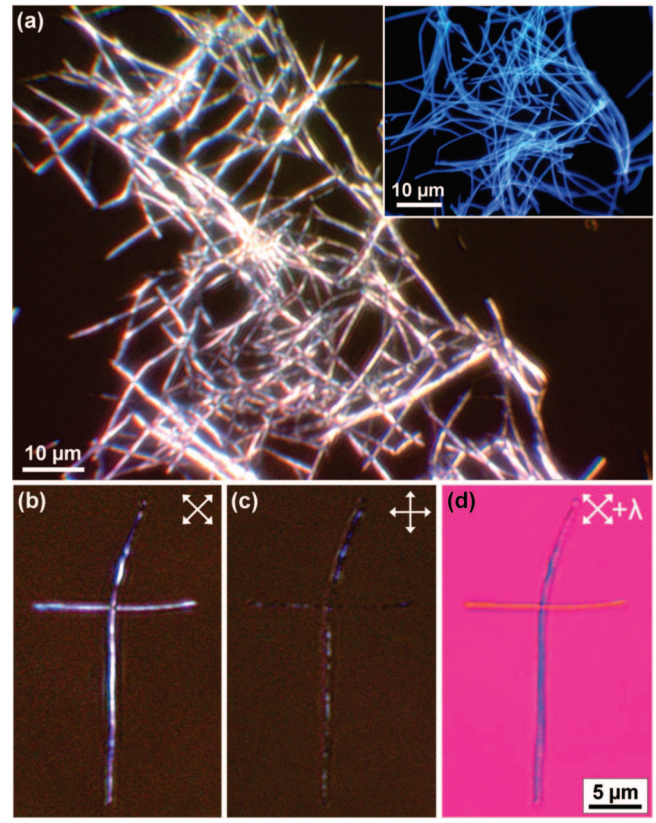

Figure 1. (a) POM image of a mat of PFO nanowires imaged through crossed polarizers. Inset: Epi-fluorescence image of a mat of PFO nanowires under UV excitation. (b−d) POM images of two crossed nanowires acquired as the sample was rotated in a plane between crossed polarizers: (b) at maximum brightness, (c) at extinction, and (d) at maximum brightness and in the presence of a 550 nm λ-retardation plate. The white arrows indicate the orientation of the crossed polarizers with respect to the wires. The slow axis of the retardation plate is vertical in (d). All nanowires were deposited on glass coverslips.

The preferred direction of polymer chain alignment in the crossed nanowire sample was determined at optimum brightness by inserting a λ-retardation plate (550 nm) between the sample and the analyzing polarizer; see Figure 1d. The slow axis of the retardation plate was oriented vertically with respect to the image reference frame. The nanowire aligned parallel to the slow axis of the retardation plate appeared blue in color against the (isotropic) magenta background

(26) Moynihan, S.; Iacopino, D.; O'Carroll, D.; Lovera, P.; Redmond, G. *Chem. Mater.* **2008**, *20*, 996.
(27) Moynihan, S.; Iacopino, D.; O'Carroll, D.; Doyle, H.; Tanner, D. A.; Redmond, G. *Adv. Mater.* **2007**, *19*, 2474.
(28) O'Brien, G. A.; Quinn, A. J.; Tanner, D.; Redmond, G. *Adv. Mater.* **2006**, *18*, 2379.
(29) Hensley, D. A. *The Light Microscopy of Synthetic Polymers*; Oxford University Press: New York, 1984.
(30) Robinson, P. C.; Bradbury, S. *Qualitative Polarized-Light Microscopy*; Oxford University Press: New York, 1992.

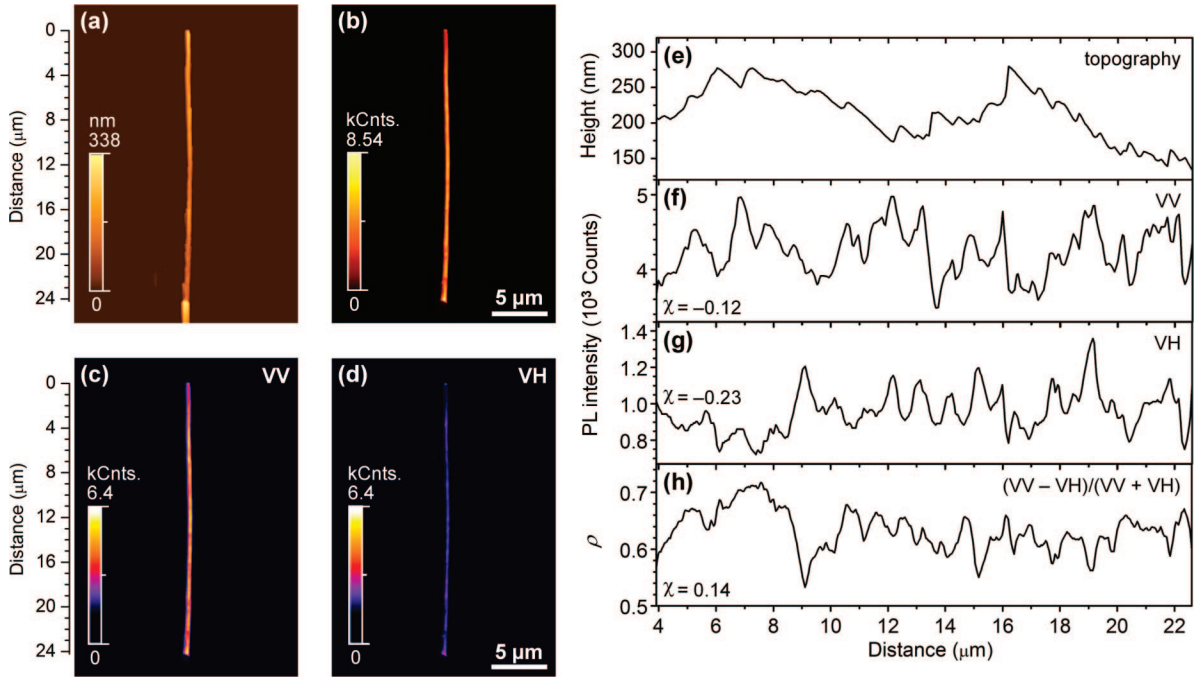

Figure 2. (a) NSOM topography image of a single PFO nanowire deposited on a glass substrate from decane suspension. The feature at the end of the nanowire is a topographic artifact. (b) Total NSOM PL intensity image of the same nanowire. (c, d) Polarization-resolved NSOM PL intensity images of the nanowire, acquired simultaneously under vertically (i.e., axially) polarized excitation with vertically (VV) and horizontally (VH) polarized collection, respectively. All images were rotated by 90°. (e) Nanowire topography line profile. (f, g) VV and VH PL intensity line profiles. (h) Polarization ratio, ρ, profile calculated as indicated. The profiles are plotted as a function of distance from one end of the nanowire, as indicated by the scale bars on (a) and (c). The cross-correlation coefficient, χ, of the topography profile with each of the VV, VH, and ρ profiles is included in each panel.

while the nanowire aligned perpendicular to the slow axis of the retardation plate appeared orange in color. By comparison with the Michel−Levy polarization interference color chart, this blue/orange polarization color contrast indicated that the PFO polymer chains were oriented vertically/horizontally in the image reference frame suggesting net alignment of the polymer chains parallel to the long axis of each wire.[29−31] Similar behavior was observed when nanowires were immersed in a high refractive index liquid (n = 1.65; Series B, Cargille-Sacher Laboratories, Inc.), indicating that dielectric confinement effects in these nanowires were negligible under white light illumination.[32] The axial polymer chain alignment was likely due to mechanical extension of the polymer chains during template pore filling and, afterward, during directional loss of solvent from the pores.[33,34] Variations in optical color contrast were occasionally observed along the length of nanowires in the POM images, possibly because of the presence of regions or domains having varying degrees of molecular orientation.

For near-field polarization-resolved PL imaging measurements of single solution-wetted PFO nanowires, a nanowire-coated glass coverslip was positioned on the NSOM stage (in air) so that the long axis of a selected wire was either vertical or horizontal in the image reference frame. Axially polarized near-field excitation at 405 nm was employed (i.e., polarized parallel to the long axis of the nanowire). A topography image and two orthogonally polarized PL images were simultaneously acquired while raster scanning the NSOM stage and keeping the NSOM probe tip within 10 nm of the sample surface using a shear force feedback control mechanism (scan rate: 30 μm s^{-1}). This permitted spatial variations in nanoscopic light emitting regions to be probed and correlated with the nanowire topography, with nominal lateral resolution down to 50 nm (determined by the aperture sizes of the NSOM probes employed). Figure 2a shows a NSOM topography image of a typical, clean, well-isolated, high aspect ratio nanowire, 24 μm in length and with an average height of 189 nm (standard deviation of 48 nm). A total NSOM PL intensity image of the wire acquired under vertically polarized excitation is shown in Figure 2b. The image showed sharp contrast between the nanowire and the background, with a full width at half-maximum (FWHM) of 210 ± 23 nm, in good agreement with the measured nanowire diameter. The absence of diffraction-limited broadening of the PL emission image confirmed the true sub-wavelength resolution of the NSOM system employed. The scan direction was vertical in images a and b in Figure 2.

Polarization-resolved NSOM PL intensity images were acquired under conditions of vertically, i.e., axially, polarized excitation with vertical (VV) and horizontal (VH) collection polarizations; see images c and d in Figure 2, respectively. The scan direction was vertical in both images. Wire emission was strongly anisotropic, being very intense when the collection polarizer was oriented parallel to the wire long axis (i.e., VV). This behavior was generally observed for solution-wetted PFO nanowires. Because the wire was

(31) Yao, H.; Domoto, K.; Isohashi, T.; Kimura, K. *Langmuir* **2005**, *21*, 1067.
(32) Wang, J.; Gudiksen, M. S.; Duan, X.; Cui, Y.; Lieber, C. M. *Science* **2001**, *293*, 1455.
(33) Bäcklund, T. G.; Sandberg, H. G. O.; Österbacka, R.; Stubb, H.; Torkkeli, M.; Serimaa, R. *Adv. Funct. Mater.* **2005**, *15*, 1095.
(34) Moynihan, S.; Lovera, P.; O'Carroll, D.; Iacopino, D.; Redmond, G. *Adv. Mater.* **2008**, *20*, 2497.

cylindrically symmetric about its long axis, and since the emission transition dipole of a conjugated polymer chain is oriented with respect to the polymer backbone by a fixed off-axis angle, β_N, this distinct emission anisotropy suggested that a significant number of the emissive polymer chains were preferentially oriented about the long axis of the nanowire, in agreement with the POM data of Figure 1 above.

To investigate the degree and extent of polymer chain orientation within the nanowire in more detail, we plotted axial line profiles extracted from the NSOM topography and polarization-resolved NSOM PL intensity images as a function of distance from the nanowire tip; see Figure 2e to Figure 2g. It was apparent that variations in both topography and polarized PL intensity occurred along the length of the wire. The topography profile along the central region of the nanowire exhibited many features ranging in height from 131 to 280 nm with a mean height of 214 nm and a standard deviation of 37 nm (i.e., ± 17%). The polarization-resolved PL intensity line profiles, denoted by VV and VH, respectively, also exhibited many features. The intensity mean and standard deviation of the measured PL signals were 4250 and 323 counts (i.e., ±8%) and 956 and 113 counts (i.e., ±12%), respectively.

The features in the topography line profile ranged in lateral extent from 130 to 900 nm, whereas features in the VV and VH PL intensity line profiles ranged in lateral extent from 80 nm to 1.2 μm. Some features correlated in the VV and VH PL intensity line profiles but anticorrelated with the topography line profile (see, for example, the features located at 7.3 and 20.4 μm from the nanowire tip), indicating that they were due either to topographic artifacts, insoluble or entangled polymer chains or impurities protruding at the surface of the nanowire (causing so-called cluster-correlated fluorescence)[35] or, possibly, to fluctuations in excitation laser power; see the Supporting Information for further details. Overall, the cross-correlation coefficients between the topography and each of the VV and VH PL intensity line profiles were determined to be −0.12 and −0.23, respectively, consistent with slight anticorrelation. Many other features in the VV and VH PL intensity line profiles were anticorrelated or uncorrelated with respect to each other while exhibiting little or no correlation with topography (see, for example, the features located at 9.1 and 11.2 μm from the nanowire tip). These features suggested the existence of domains of long-range order within the nanowire,[35] likely associated with regions having varying degrees of polymer chain alignment. The physical extent of these domains was difficult to determine directly from the VV and VH PL intensity line profiles because the data was convoluted with features caused by measurement artifacts and/or cluster-correlated fluorescence, as described above.

To eliminate the effects of such measurement artifacts and cluster-correlated fluorescence from the measured data, a line profile of polarization ratio, ρ, was calculated, where $\rho = (I_{VV} - I_{VH})/(I_{VV} + I_{VH})$, ($I_{VV}$ and I_{VH} are the PL intensities measured for each polarization condition); see Figure 2h. Values for ρ varied from 0.53 to 0.72 with a mean value of 0.63 and a standard deviation of 0.036 (i.e., ± 6%). The relatively large positive values for ρ were consistent with preferential alignment of emissive polymer chains about the long axis of the nanowire. The ρ line profile exhibited an overall positive cross-correlation coefficient with topography ($\chi = 0.14$) indicating that PL intensity features which anticorrelated with topography were effectively suppressed using this analysis method. As a result, using this approach, domains within the nanowire of up to 2 μm in size and exhibiting excellent polymer chain alignment could be resolved without contributions from measurement artifacts or cluster-correlated fluorescence.

Polarization-resolved PL spectra were acquired at various points along the wire following near-field excitation; see Figure 3, left panel and Figure 3a−e. For these measurements, the probe was held stationary at a particular point while each of the VV and VH spectra were collected. VV spectra exhibited peaks located at 446, 470, and 503 nm, assigned to the $S_1 \rightarrow S_0$ 0−0 transition of β-phase PFO with 0−1, 0−2 vibronic replicas, respectively.[22] VH spectra exhibited slightly blue-shifted peaks located at approximately 443, 468 and 501 nm, respectively. In addition, the FWHM of the VV spectral peaks were consistently smaller than those of VH spectra (0−1 and 0−2 peaks exhibited average FWHM of 95 and 93 meV, respectively, for VV spectra and 108 and 104 meV, respectively, for VH spectra). Clipping of the 0−0 peak in the VV spectra was attributed to a polarization bias in the collection optics below 435 nm. The long wavelength features (above ~520 nm) were attributed to unresolved vibronic replicas and fluorenone defect emission.[36,37] Emission intensity was always greater for VV spectra, indicating that the emissive β-phase chains were preferentially aligned about the long axis of the nanowire, in agreement with the PL image data of Figure 2. Emission dichroic ratios, I_{VV}/I_{VH}, of between 4.6 and 8.9 were determined, consistent with a preferred axial orientation of the β-phase emitters with variations in the degree of polymer chain alignment along the wire length.

The insets to Figure 3a−e show plots of polarization ratio, ρ, calculated from the measured spectra as a function of emission wavelength. Values of ρ of between 0.64 and 0.83 were determined at the various measurement locations, indicating strong axial emission anisotropy. For each polarization condition, ρ did not decrease significantly with increasing wavelength, suggesting that the same population of chromophores was responsible for emission at all wavelengths (i.e., that complete excitation energy transfer from the g-phase to the β-phase had occurred) and, hence, that depolarization of emission was absent.[38] Furthermore, slight increases in ρ were apparent at the red edge of each spectral peak, arising from the slightly red-shifted and narrowed nature of the VV spectra relative to the VH spectra. This observation suggested that the axially aligned emissive β-phase polymer chains had slightly longer conjugation

(35) Teetsov, J.; Vanden Bout, D. A. *J. Phys. Chem. B* **2000**, *104*, 9378.
(36) Becker, K.; Lupton, J. M.; Feldmann, J.; Nehls, B. S.; Galbrecht, F.; Gao, D.; Scherf, U. *Adv. Funct. Mater.* **2006**, *16*, 364.
(37) Sims, M.; Bradley, D. D. C.; Ariu, M.; Koeberg, M.; Asimakis, A.; Grell, M.; Lidzey, D. G. *Adv. Funct. Mater.* **2004**, *14*, 765.
(38) Clark, A. P.-Z.; Shen, K.-F.; Rubin, Y. F.; Tolbert, S. H. *Nano Lett.* **2005**, *5*, 1647.

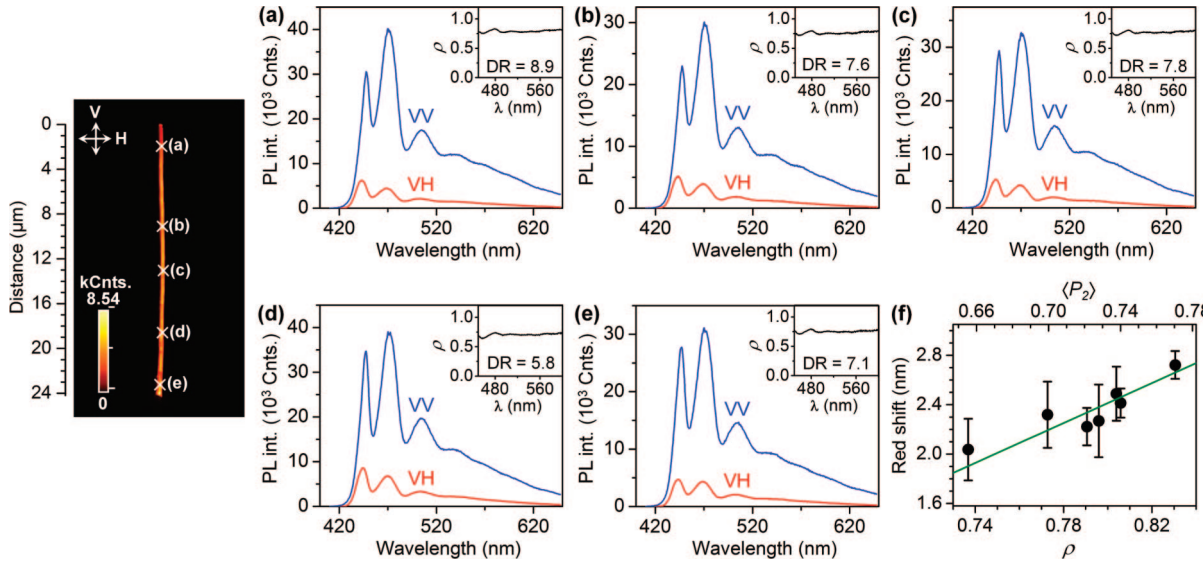

Figure 3. Left panel: Total NSOM PL intensity image of Figure 2b. (a−e) Polarization-resolved NSOM PL spectra acquired at various locations along the length of the nanowire of Figure 2. The locations on the wire from which the spectra were acquired are indicated in the left panel. The insets in a−e are plots of the polarization ratio, ρ, calculated versus wavelength. The corresponding emission dichroic ratios measured at the 0−1 peak, DR, are also included. (f) Plot of the red shift of the 0−1 peak versus ρ determined from multiple polarization-resolved NSOM PL spectra (black circles). $\langle P_2 \rangle$ values calculated using ρ as described in the main text are included on the upper scale. The red shift was systematically determined by multiple Gaussian fitting of each spectrum to determine the 0−1 peak position and subsequent subtraction of the 0−1 peak positions of corresponding VV and VH spectra. The green line is a linear fit to the data and the error bars are the Gaussian fit error.

lengths (i.e., lower energies) than chains having other orientations,[39,40] further suggesting that axially aligned β-phase chains could act as relatively more efficient excitation energy traps. Figure 3f is a plot of the red shift in VV spectra with respect to VH spectra measured at various locations along the nanowire as a function of ρ. The red shift increased linearly with increasing value of ρ, a result that further supported the assertion that strongly axially oriented β-phase chains have the longest conjugation lengths.

To better quantify the degree of local β-phase chain alignment within the nanowire, values for the orientational order parameter, $\langle P_2 \rangle = 1/2\langle 3\cos^2\theta - 1 \rangle$, which is often used to quantify the extent of molecular order in organic systems, were estimated (where θ represents the angle made between an emitting polymer chain and the nanowire long axis; see Figure 4a). $\langle P_2 \rangle = 1$ for perfect molecular alignment with respect to a selected direction; $\langle P_2 \rangle = 0$ for isotropic alignment and $\langle P_2 \rangle = -0.5$ for perpendicular alignment with respect to the selected direction. To extract $\langle P_2 \rangle$ values from the measured polarization-resolved NSOM PL data, the expression $\langle P_2 \rangle = (2\rho/(3 - \rho))/(1/2\langle 3\cos^2\beta_N - 1 \rangle)$ was employed, where β_N represents the angle made between the emission transition dipole and the polymer chain axis (Figure 4a) and the brackets, $\langle\ \rangle$, denote an ensemble average over all emitting chains.[41] Concerning selection of a value of β_N for the β-phase emitters, the off-axis transition dipole angle of PFO chains in thin glassy films of PFO aligned in the nematic mesophase on rubbed polyimide has been determined by Gather et al. to be 21 ± 3^o from Raman anisotropy

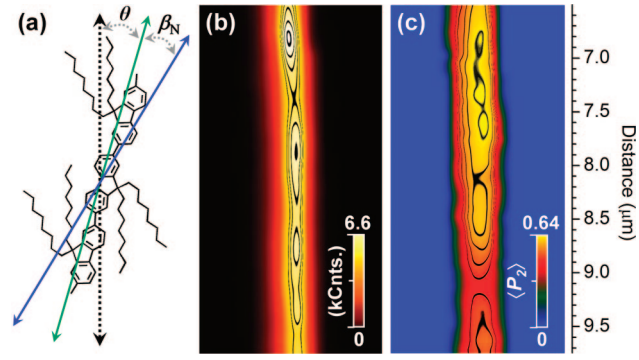

Figure 4. (a) Simplified schematic depiction of three PFO monomer units. The dashed black line represents the nanowire long axis. The solid green line represents the axis of the polymer chain making an angle, θ, relative to the nanowire long axis. The solid blue line represents the axis of the emission transition dipole making an angle, β_N, relative to the axis of the polymer chain. (b) Total NSOM PL intensity image of a section of the nanowire of Figure 2. (c) $\langle P_2 \rangle$ image map of the same section of the wire. The black lines in (b) and (c) are contours with spacing of 0.43 k counts and 0.032, respectively.

measurements.[42] However, the off-axis transition dipole angle of β-phase PFO has not been experimentally determined due to the difficulty of aligning a significant faction of this phase in thin films without employing thermal treatment protocols that would otherwise destroy the phase.[21] It is likely, however, that the off-axis transition dipole angle of β-phase PFO is smaller than that of the other PFO phases since it is relatively more planar and exhibits large intrachain correlation lengths (~22 nm, i.e., 24 monomer repeat units).[22] In this regard, Hagler et al. employed the analytical expression $\tan(\beta_N) = 1/(N^{1/2})\tan(\beta_0)$ to estimate the off-axis transition dipole angle of a conjugated polymer chain, β_N, as a function of its excited-state localization length, N, and the off-axis transition dipole angle of a single monomer unit,

(39) Herz, L. M.; Phillips, R. T. *Phys. Rev. B* **2000**, *61*, 13691.
(40) Tsoi, W. C.; Charas, A.; Cadby, A. J.; Khalil, G.; Adawi, A. M.; Iraqi, A.; Hunt, B.; Morgado, J.; Lidzey, D. G. *Adv. Funct. Mater.* **2008**, *18*, 600.
(41) Lakowicz, J. R. *Principles of Fluorescence Spectroscopy*, 2nd ed.; Kluwer Academic/Plenum Publishers: New York, 1999.
(42) Gather, M. C.; Bradley, D. D. C. *Adv. Funct. Mater.* **2007**, *17*, 479.

β_0, based on a simplified analysis of its molecular structure.[43] Using this approach, and taking $N = 24$ and $\beta_0 \approx 19^o$,[21,22,44] β_N was estimated at $\sim 4^o$ for β-phase PFO. Therefore, taking the range of ρ values determined from the polarization-resolved PL spectra of Figure 3, and selecting a value of $\beta_N = 4^o$ for the β-phase emitters, local values for $\langle P_2 \rangle$ were determined to range from 0.47 to 0.76, consistent with the existence of domains within the nanowire having different degrees of emissive β-phase polymer chain alignment (with respect to the long axis of the wire); see Figure 3f.

To visualize the extent of β-phase chain alignment, the polarization-resolved NSOM PL intensity images of Figure 2c and Figure 2d were combined to generate a spatial $\langle P_2 \rangle$ image map of the wire, according to the expression for $\langle P_2 \rangle$ defined above with respect to ρ and β_N. Before performing the image math, the noise floor was subtracted from both images to eliminate noise from the calculation and, subsequently, 1 count was added to the VH image to avoid division by 0. The resulting image spatially represented $\langle P_2 \rangle$ with a lateral resolution of about 80 nm. Employing ρ to locally determine $\langle P_2 \rangle$ in this manner substantially reduced the contribution of artifacts to the final $\langle P_2 \rangle$ image.[35] Figure 4b shows a total NSOM PL intensity image for a region of the nanowire with intensity contours included in order to highlight small variations in PL intensity along the wire. Slight variations in PL intensity were apparent with a standard deviation of 330 counts (i.e., $\pm$ 6%). Figure 4c shows the $\langle P_2 \rangle$ image map of the same region of this wire. The color scale in the image ranged from blue, indicating no order ($\langle P_2 \rangle = 0$), to yellow, indicating a high degree of chain alignment with respect to the nanowire long axis ($\langle P_2 \rangle = 0.64$). Ordered domains of up to $\sim$ 1.5 μm in size with $\langle P_2 \rangle$ values between 0.48 and 0.64 were apparent along this section of the nanowire (red to yellow color), with $\langle P_2 \rangle$ mean and standard deviation of 0.57 and 0.06 (i.e., $\pm$ 10.5%), respectively, being determined. By analyzing axial line profiles extracted from images b and c in Figure 4, features in the $\langle P_2 \rangle$ data were found to exhibit negligible correlation with features in the total PL intensity data (cross-correlation coefficient, χ, of 0.03 for the wire), indicating that variations in aperture-nanowire distance (i.e., topographic artifacts), cluster-correlated fluorescence or fluctuations in laser excitation power did not contribute significantly to $\langle P_2 \rangle$. Using this approach, domains of long-range order of up to 2 μm in size exhibiting $\langle P_2 \rangle$ values in the range of 0.47−0.76, and with $\langle P_2 \rangle$ mean and standard deviation of 0.54 and 0.036 (i.e., $\pm$ 7%), respectively, were resolved along the full length of the nanowire.

Note that the values of $\langle P_2 \rangle$ determined in this study, although large, were expected to be slightly underestimated for the following reasons: First, considering the extinction coefficient of PFO ($\sim 2 \times 10^5$ cm^{-1} at 405 nm),[45] a nanowire would be expected to absorb most of the excitation light delivered from the NSOM probe aperture within a depth of 50 nm from its top surface. However, in the measurement configuration employed, nanowire emission was collected in the far-field, i.e., from the opposite side of the wire to that excited by the NSOM probe (transmission mode), and, as a consequence, most of the nanowire body extended beneath the excitation zone into the far-field. Because it was necessary for near-field excited PL emission to pass through the wire body prior to collection in the far-field, PFO domains within the nanowire body having different net molecular orientations could have acted as emission depolarizers, thereby reducing the magnitudes of extracted values of $\langle P_2 \rangle$.[35] Second, because the intrachain correlation length of a β-phase PFO chain is $\sim$22 nm,[22] some of the domains detected by the NSOM may have actually been ensembles of smaller domains having higher degrees of alignment but with slightly different relative orientations. Domains of this size would have been below the lateral resolution of the system and, consequently, the degree of local polymer chain alignment estimated from the NSOM data would have been underestimated in such cases.[35] Third, the degree of linear polarization of the excitation light delivered from the NSOM probe aperture was only 7:1. As a result, the population of emissive polymer chains contributing to the signals collected during the polarization-resolved NSOM PL measurements may have possessed broader orientation distributions than ideally desired and, consequently, the magnitudes of the emission polarization ratios calculated using such data could have been underestimated. Fourth, because a high numerical aperture collection objective (NA = 1.25) was employed for PL collection, all emission within a full collection cone angle of 110^o was detected (NA = $n \times \sin \sigma$; where n is the refractive index of the immersion oil and σ is the maximum half angle subtended by the objective as viewed from the sample).[46] In this situation, emission polarization ratios calculated from the measured PL intensity data were likely to have been underestimated because of slight depolarization of the PL signals by mixing of the V and H emission polarization components associated with out-of-plane projections of the emission dipoles.

Conclusions

In conclusion, poly(9,9-dioctylfluorene) nanowires were fabricated by solution-assisted wetting of anodic alumina templates. Nanowires exhibited pronounced optical birefringence when observed between crossed polarizers. Detailed polarized optical microscopic analysis indicated axial alignment of polymer chains within the wires. The impact of this internal polymer chain alignment on the emissive properties of single wires was investigated using polarization-resolved near-field photoluminescence imaging and spectroscopy methods. In this manner, spatial variations in nanoscopic light emitting regions along a nanowire could be probed and correlated with nanowire topography with a nominal lateral resolution of 50 nm. Polarization-resolved near-field emission intensity images of single wires exhibited strongly anisotropic luminescence with a preferred axial polarization suggesting that a significant number of the emissive polymer chains were

(43) Hagler, T. W.; Pakbaz, K.; Heeger, A. J. *Phys. Rev. B* **1994**, *49*, 10968.
(44) Liem, H.-M.; Etchegoin, P.; Whitehead, K. S.; Bradley, D. D. C. *Adv. Funct. Mater.* **2003**, *13*, 66.
(45) Campoy-Quiles, M.; Heliotis, G.; Xia, R.; Ariu, M.; Pintani, M.; Etchegoin, P.; Bradley, D. D. C. *Adv. Funct. Mater.* **2005**, *15*, 925.
(46) Axelrod, D. *Biophys. J.* **1979**, *26*, 557.

preferentially oriented about the long axis of each nanowire. Polarization-resolved near-field emission spectra acquired at multiple locations along the length of a single wire indicated that the more planar, extended β-phase polymer chain conformation of PFO dominated the wire emission and confirmed that the β-phase luminescence was strongly anisotropic with emission dichroic ratios of between 4.6 and 8.9 being determined. To visualize the extent of β-phase polymer chain alignment within a typical nanowire, we generated image maps of the orientational order parameter, $\langle P_2 \rangle$, from measured near-field emission intensity image data. Using this approach, numerous domains of long-range order of up to 2 μm in size with $\langle P_2 \rangle$ values ranging from 0.47−0.76 were identified, indicating extensive axial alignment of the emissive β-phase chains within the nanowires. It is anticipated that the anisotropic optical properties of these novel conjugated polymer nanowires will be useful for the realization of future subwavelength organic devices with controllable electrical and optical properties.

Acknowledgment. This work was supported by the Irish HEA PRTLI Nanoscience and IRCSET Embark initiatives and by the EC "Nano3D" project.

Supporting Information Available: Discussion of topographic artifacts, cluster-correlated fluorescence, and long-range order in polarization-resolved near-field scanning optical microscopy photoluminescence data; data analysis approach employed to distinguish long-range order from topographic artifacts and cluster-correlated fluorescence in near-field optical microscopy data (PDF). This material is available free of charge via the Internet at http://pubs.acs.org.

CM8015534